



Cite this: DOI: 10.1039/d5fb00391a

Effect of pin-to-plate atmospheric pressure cold plasma on mustard protein isolate: physicochemical, structural, thermal, and functional characterization

Fizah Farooq,^a Toiba Majeed,^a Sharath Kumar Nagaraja^{ab} and Aamir Hussain Dar  ^a

The present work was aimed at studying the physicochemical, structural, functional, and thermal impact of atmospheric pressure cold plasma on mustard protein isolates. The mustard protein isolate was treated at selected voltage levels (10 and 20 kV) exposed for 5 and 10 min, resulting in a non-significant increase in water absorption capacity and oil absorption capacity in all treated samples. There was a significant increase ($p < 0.05$) in the emulsification (20 kV for 10 min –47.81%) and foaming (20 kV for 5 min –59.77%) properties of the treated protein isolates, which underscores the process-induced improvement in interfacial properties due to unfolding and partial denaturation. With respect to solubility, the solubility of the treated protein isolate (20 kV for 20 min) increased to 43.97%, which was due to the reactive species opening up the active sites responsible for hydration. Overall, the study revealed the potential impact of cold plasma on a non-conventional protein isolate and showed that plasma treatment at 10 kV for 10 min had an improving yet balanced effect on the hydration, solubility and surface-active properties that may find space in both food and non-food applications.

Received 17th July 2025

Accepted 3rd September 2025

DOI: 10.1039/d5fb00391a

rsc.li/susfoodtech

Sustainability spotlight

The present study provides a pathway for technological valorisation of mustard seed meal, a major by-product from the edible oil industry. In the era of exploring non-conventional and plant-based proteins for human nutrition, this research provides a sustainable utilisation method suitable for a circular economy. Mustard seed meal post oil extraction serves as a promising source for plant-based proteins with a rich amino acid composition. Non-thermal technology such as cold plasma is being used to modify and improve the techno-functional properties of native mustard protein isolate. The employed treatment conditions were able to bring an improvement in solubility, hydration, emulsification and foaming properties, which are desirable attributes required by the food industry. Overall, the work aligns with sustainable development goals by focusing on a circular economy, improving resource use efficiency, and the transition towards green protein production with clean label claims that are collectively aimed at building a sustainable and resilient food ecosystem.

1 Introduction

Proteins, polymeric biomolecules composed of amino acid monomers, occupy a greater dietary significance in present-day food systems. In addition to their nutritional potential, the biomolecules, also exhibit important techno-functional properties that make them valuable ingredients in the food industry. The gelling, emulsifying, foaming and hydration properties of proteins contribute greatly to formulating and stabilizing various food colloidal systems. The molecules are extremely sensitive to temperature, pH and process conditions, leading to denaturing, which thereby alters the corresponding functionality. In brief, the structural composition of proteins tends to

dictate their functionality, which successively drives their innovative applications. Plant-derived proteins have emerged as an alternate protein source that contributes to sustainability and the march towards resilient food systems. There are various sources of plant-based proteins, including cereals, legumes, oilseeds, nuts, fruits, vegetables, and algae, that have been explored as nutritional, functional and techno-commercial alternatives to animal proteins. Of the mentioned protein sources, oilseed meal, which contains abundant protein, has been in focus during recent years as the defatted biomass holds significant potential to meet the protein requirements of present-day food systems.

Mustard oil is a widely used edible cooking oil owing to its peculiar flavour, pungent profile and relatively good composition of unsaturated fatty acids. The oilseed meal by-product post cold pressing or solvent extraction hosts major macromolecular composition that makes this by-product a greater source for protein, extraction, quantification and utilisation. Defatted

^aDepartment of Food Technology, Islamic University of Science & Technology, Kashmir, India. E-mail: daraamirf@gmail.com

^bICAR-Central Institute of Temperate Horticulture, Srinagar, Kashmir, India. E-mail: sharath16.icar@gmail.com



oilseed meal is known to contain around 18–24% protein and has a balanced amino acid composition.¹ The food application of mustard protein was investigated by Pucean *et al.*,² who found the 7% substitution with wheat flour provides bread with higher nutritional and organoleptic acceptance. Similarly, in the non-food segment, Hendrix *et al.*³ considered using defatted mustard seed meal as a base material for biodegradable film fabrication. By underscoring the nutritional benefits of mustard protein, this work highlights its potential contribution to the global food system in meeting the protein dietary requirements. However, as proteins in their native state are not suitable for industrial processing requirements, it becomes essential to modify the native state to improve various functional benefits without lowering the nutritional density. Non-thermal treatments applied to proteins give the positive effects of reduced denaturation, minimal impact on nutritional profile, reduced color loss, and beneficial changes to the protein structure by limiting adverse cross-linking and aggregation. In addition, resorting to non-thermal approaches would drastically reduce the energy expenditure and associated negative impact on isolated proteins.

Cold-plasma-mediated protein modification has garnered growing interest in the scientific community as a means to selectively modify the functional properties of proteins without compromising their structural integrity.^{4,5} The reaction between partly or fully ionized gas molecules with the protein molecule of interest leads to partial unfolding, peptide bond cleavage, disulfide bond formation, changes in surface hydrophobicity and cross-linking reactions.⁶ By altering engineering variables such as voltage, duration of treatment, and frequency, it is possible to tune and optimize proteins with desirable functionality. As the interest in protein fortification resulting in functional food product development is rising, it becomes important to modify native proteins to improve the functional benefits without disturbing the nutritional composition. Mustard, as a host of high-quality proteins, is a promising candidate to be improved upon and driven across food applications. Second, the abundance of this crop supports commercial-scale production, as mustard is the third-largest oilseed after soybean and palm. It is very important that this huge biomass needs to be sustainably trapped for its valuable protein resource and made available for the future plant-based protein segments. Until now, various works have been undertaken to improve the recovery, yield efficiency, and purity of mustard protein concentrates and isolates.^{1,7} Some of the investigations have explored the use of mustard protein isolates in pasta formulations, where up to 5% of refined flour was substituted with mustard protein isolate; beyond this level, the dough exhibited a loss in maximum consistency index.⁸ To increase the food application space of mustard protein isolate, hardly any studies were found on the modification of native proteins and, in particular to the best of the authors' knowledge, no studies have investigated the effects of cold plasma modification on mustard protein isolate. Therefore, this study evaluates the effects of the selected treatment conditions (voltage and duration) on mustard protein isolate and further characterizes the physicochemical, structural, functional, and thermal properties of the modified protein.

2 Materials and methods

2.1 Materials

Mustard seed meal was procured from a nearby mustard oil processing company, Srinagar, J&K. It was immediately defatted using *n*-hexane. The defatted meal was packed in airtight LDPE bags and stored at 4 °C until use. All the chemicals were procured from Hi-Media (India) and were of analytical grade.

2.2 Preparation of mustard protein isolates

The protein extraction from defatted mustard meal was carried out as per the procedure of Jahan *et al.*⁹ with certain modifications. The defatted and finely ground mustard seed meal was mixed with distilled water (1:10) and continuously stirred using a magnetic stirrer. During stirring, the pH of the mixture was adjusted to pH 11 (selected based on preliminary experiments, which resulted in increased extraction yield) using 1 N NaOH. The suspension was then centrifuged at 8000 × *g* for 20 min at 4 °C. The pH of the obtained supernatant was adjusted to 4.5 using 0.1 N HCl, followed by a second centrifugation at 8000 × *g* for 20 min at 4 °C. The supernatant was discarded, then the sediment was collected, washed twice with distilled water and freeze-dried (−80 °C for 24 h). The dried protein isolates were finely ground using a laboratory mixer and packed in airtight polyethylene bags. The bags were stored at 4 °C until use.

2.3 Chemical analysis of mustard protein isolate

2.3.1 Proximate composition of MPI. Moisture, total ash, crude protein, crude fat and crude fibre of the native (defatted seed meal) and isolated mustard protein were analysed following AOAC methods.¹⁰ Protein content was determined by multiplying the nitrogen content by a factor of 6.25. The carbohydrate content was calculated by subtracting the values of moisture, ash, protein and fat from 100.

2.3.2 Color properties of MPI. The color properties (*L**, *a**, *b**) for the defatted mustard meal and MPI were analysed using a precalibrated Hunter Lab colorimeter (Color Flex EZ Model no. 45/0) following the procedure of Ge *et al.*¹¹ The readings gave the values for *L** (0 is black and 100 is white), *a** (+red and −green) and *b** (+yellow and −blue). The chroma (*C*) and hue angle were calculated based on the obtained color coordinates.

$$C = \sqrt{a^{*2} + b^{*2}}$$

$$\text{Hue angle} = \tan^{-1}(b^*/a^*)$$

where *L**, *a**, and *b** are the color values for the sample and *L*, *a*, and *b* are the color values for the reference white tile.

2.4 Atmospheric pressure cold plasma treatment of mustard protein isolates

Atmospheric pressure cold plasma treatment was carried out using a multipin discharge plasma reactor (IN-HVLT MP, Ingenium Naturae Private Limited, Gujarat, India) with an input



voltage of 230 V, frequency set to 50 Hz and current set to 5 mA. The cold plasma reactor had 63 high-voltage pins with a dischargeable area of $1.85 \times 2.5 \text{ cm}^2$. The presence of electrode pins and fringes tends to maintain the voltage. Mustard protein isolate samples were placed in a 90 mm Petri plate with a thickness maintained at 2 mm. The selected voltage (10 and 20 kV) was based on preliminary studies, and the treatment duration was fixed at 5 and 10 min, respectively. Therefore, the work had four treatments: T1 (10 kV for 5 min), T2 (10 kV for 10 min), T3 (20 kV for 5 min) and T4 (20 kV for 10 min). Throughout the experiment, a uniform electrode distance (3 cm) was maintained.

2.5 Physicochemical properties

2.5.1 Water absorption capacity (WAC). The WAC for the control and treated protein isolate was determined using the procedure reported by Ji *et al.*¹² with certain modifications. Briefly, 1 g of sample (W_1) was allowed to hydrate with 10 mL of distilled water (W_2), then mixed thoroughly and centrifuged at $3000 \times g$ for 15 min. The supernatant was carefully removed, and the decanted mass was weighed (W_3). The WAC was calculated as per the formula:

$$\text{WAC} = \frac{W_3 - W_2}{W_1} \times 100$$

2.5.2 Oil absorption capacity (OAC). The OAC for the control and treated protein isolate was determined using the procedure reported by Stone *et al.*¹³ with certain modifications. A 0.5 g sample (W_1) was taken in a centrifuge tube and mixed with 5 mL of sunflower oil using a vortex mixer (W_2). The suspension was centrifuged at $3000 \times g$ for 15 min. The supernatant was discarded, and the sediment weight was noted (W_3). The OAC was expressed as grams of sunflower oil held by the suspension.

$$\text{OAC} = \frac{W_3 - W_2}{W_1} \times 100$$

2.5.3 Emulsifying absorption capacity (EAC). The emulsifying capacity of the treated and control samples was determined using the method reported by Nawaz *et al.*¹⁴ with some modifications. To a graduated centrifuge tube, 50 mg of sample was added. To the sample, 5 mL of distilled water was added. After vortexing for a while, 5 mL of soybean oil was added to the sample and mixed thoroughly. The emulsion was centrifuged at $3000 \times g$ for 5 min at 4 °C, after which the developed emulsion layer was precisely measured (V_2) and the total volume of suspension was recorded (V_1). The EAC is calculated with the following equation:

$$\text{EAC} = \frac{V_2}{V_1} \times 100$$

2.5.4 Emulsifying stability index (ESI). The ESI for the native and CP-treated MPI was analysed following the procedure of Kuan and Liong.¹⁵ The emulsion was prepared (V_2) as

mentioned in Section 2.3.1 and heated in a water bath maintained at 80 °C for 30 min. The heated emulsion was immediately cooled to room temperature (25 °C) and then centrifuged ($3000 \times g$) for 10 min. The final volume (V_3) was measured and used for the calculation of the ESI.

$$\text{ESI} = \frac{V_3}{V_2} \times 100$$

2.5.5 Foaming capacity (FC). By minor modification of the methodology of Kang *et al.*,¹⁶ the FC of the samples was determined. A 1 g sample was homogenized with 50 mL of distilled water and the initial height of the suspension was taken (V_1). The suspension was then foamed using a homogenizer at 8000 rpm for 2 min, then immediately transferred to a measuring cylinder. The height of the developed foam was noted (V_2) and the FC was calculated using the equation:

$$\text{FC} = \frac{V_2 - V_1}{V_1} \times 100$$

2.5.6 Foaming stability (FS). Foaming stability was calculated by adopting the procedure of Barac *et al.*¹⁷ The foam developed (V_1) in the graduated centrifuge tube was allowed to remain static for 30 min. The final volume was recorded (V_2) and applied to the formula to derive the FS.

$$\text{FS} = \frac{V_2}{V_1} \times 100$$

2.6 Protein solubility

The solubility of the control and cold-plasma-treated samples was analysed by applying some modifications to the method from Ji *et al.*¹² A 3% suspension of the samples was prepared with deionised water (pH 7), mixed well with vortexing, and centrifuged at $4500 \times g$ for 15 min at 20 °C. The resulting supernatant with protein molecules was reacted with biuret reagent, and the solubility was calculated using the following equation:

Protein solubility =

$$\frac{\text{protein in supernatant after reaction with reagent}}{\text{initial concentration of protein in sample}} \times 100$$

2.7 Free sulphydryl content

The proportion of free sulphydryl groups in the native and CP-treated MPI was determined following the procedure of He *et al.*¹⁸ 4 mg of DNTB (5,5'-dithiobis(2-nitrobenzoic acid)) was dissolved in 1 mL of Tris-glycine buffer (pH 8). The native and CP-treated MPI (1 µL) were mixed with 50 µL of prepared reagent, shaken well and incubated for 30 min in a water bath maintained at 25 °C. The aliquot of the mixed reagent was then centrifuged at $9000 \times g$ for 25 min at 4 °C. The supernatant was carefully collected, and the absorbance at 412 nm was recorded in a double-beam spectrophotometer (UV-vis, L1-2904). The



absorbance was used for the calculation of the free sulphydryl groups with the molar extinction coefficient of 13 600 mol L⁻¹ cm⁻¹.

2.8 Differential scanning calorimetry

The thermal profile of the native and modified protein isolates was determined using a differential scanning calorimeter (DSC-60A, Shimadzu Inc., Japan) following the procedure of Kaushik *et al.*¹⁹ Samples of approximately 2 mg were dissolved in 10 µL of 0.1 M phosphate buffer (pH 7) and placed in aluminium pans, then tightly sealed and analysed, with an empty aluminium pan used as a reference. The samples were then subjected to heating and cooling cycles at a rate of 10 °C per minute in the range from 30 °C to 180 °C. The analysis was conducted using nitrogen (99.999% purity) as the purging gas with the flow rate maintained at 20 mL min⁻¹. The peak denaturation temperature (T_d) and the enthalpy (ΔH) of denaturation were recorded.

2.9 Fourier transform infrared spectroscopy

FT-IR was employed to characterise the bonds and secondary structure of the native and CP-treated mustard protein isolate using a Spectrum-2 spectrometer (PerkinElmer, USA). The method reported by Hadnadev *et al.*²⁰ was used with certain modifications. A 200 mg sample was dispersed in 800 µL of distilled water and analysed over the spectral transmission range from 4000 to 600 cm⁻¹ with a resolution of 4 cm⁻¹. The spectra were acquired at room temperature. The secondary structure (α helix, β sheet, β turn, and random coil) was thereafter calculated in the spectral region of 1700–1600 cm⁻¹ using second-order derivation, after which Gaussian multiple peak fitting was used to calculate the protein secondary structure using Origin Pro Software (9.5, Northampton, MA, USA).

2.10 X-ray diffraction

The diffractogram patterns of the CP-treated protein samples were obtained by following the procedure of Saini *et al.*²¹ using an X-ray diffractometer (D8 Advance, Bruker, Germany). The samples were scanned from 5° to 55° at a scan rate of 1.20° min⁻¹ with a step size of 0.05°.

2.11 Scanning electron microscopy (SEM)

SEM (JEOL, Model JSM-6390 LV, Japan) was used to characterise the microstructures of the native and CP-treated protein isolates. The freeze-dried samples were ground, placed on an aluminium stub, adhered to conductive sticky tape, and coated with a thin layer of gold. Micrographs were taken at an

acceleration voltage of 15 kV at 500 \times and 1000 \times magnification for morphological characterisation.

2.12 Statistical analysis

The collected data were statistically analysed using a one-way ANOVA to compare means using SPSS (IBM version 25), and significance in the sample set was compared at $p < 0.05$ by *post hoc* Duncan test. All the experiments were conducted in triplicate, and the data is presented as mean \pm standard deviation (mean \pm SD). The interrelations among the variables and the efficacy of the treatments were studied using principal component analysis (PCA) using Origin 2019 software.

3 Results and discussion

3.1 Chemical profile of defatted mustard seed meal and MPI

3.1.1 Proximate composition of defatted mustard seed meal and native MPI. The proximate compositional difference between the defatted mustard seed meal and MPI is presented in Table 1. The defatted meal had crude protein, crude fibre and carbohydrate at 37.05, 7.22 and 43.42% respectively. Banerjee *et al.*²² reported slightly lower values for protein and carbohydrate at 32.76 and 24.86%, which are 11.57 and 42.74 times lower, respectively, as compared with the obtained results for the analysed defatted mustard meal. This difference in the major macromolecular composition could be due to varietal differences. The lower fibre content of 7.22% as compared with the 31.8% observed by Pedroche *et al.*²³ corresponds to a greater protein concentration and its digestibility. With respect to moisture, we observed a lower moisture content of 5.69%, which is well below the critical limit of 12% to have a reasonable shelf life.²⁴ A higher ash content (5.47%) reveals a greater mineral composition, which is similar to the results reported by Kaur *et al.*²⁵

Defatting by *n*-hexane lowered the fat content (1.15%) as compared with the mustard seed meal (40–41%), indicating the efficacy of the selected solvent in extracting a higher oil load. The lower the residual fat content in the defatted product, the better the selected solvent's ability to lower the lipid–protein interface. The MPI had moisture and ash contents of 4.35 and 0.23%, respectively, which are similar but slightly higher as compared with the results of Jahan *et al.*⁹ A higher crude protein content (90.23%) for MPI indicates the greater solubilisation of proteins in the defatted mustard meal, which was possible by greater solubilisation at alkaline pH and eventual electrostatic repulsion. While performing the alkaline solubilisation at different pH levels (9, 9.5, 10, 10.5 and 11), a higher yield was recorded at a higher pH (pH 11). The obtained observations

Table 1 Proximate composition of defatted mustard seed meal and mustard protein isolate^a

Sample	Moisture (%)	Water activity	Ash (%)	Crude protein (%)	Crude fat (%)	Crude fiber (%)	Total carbohydrate (%)
Defatted mustard seed meal	5.69 \pm 0.42	0.44 \pm 0.009	5.47 \pm 0.31	37.05 \pm 1.13	1.15 \pm 0.13	7.22 \pm 0.32	43.42 \pm 1.14
Mustard protein isolate	4.35 \pm 0.19	0.26 \pm 0.005	0.23 \pm 0.05	90.23 \pm 1.19	0.021 \pm 0.007	ND	5.19 \pm 0.28

^a Values are presented as mean \pm standard deviation.



were in agreement with the results reported by Mir *et al.*²⁶ in pseudocereals (*Chenopodium quinoa* and *Chenopodium album*). The higher pH levels of 10.5 and 11 provided higher yields, but it adversely affected the protein quality as some of the nitrogen had converted to non-protein nitrogenous forms and reduced the protein content. The reduction could also be due to a denaturation effect at more alkaline pH, resulting in aggregation.²⁷ Exposure of proteins to more alkaline conditions may also lead to lysinoalanine formation and introduce toxic molecules in the protein isolates.

3.1.2 Color profile of defatted mustard seed meal and native MPI. The color profile results for the defatted mustard seed meal and MPI are presented in Table 2, and calculations were done to assess the total color difference, chroma and hue angle. The large-scale market adoption of any proteins primarily relies on them having an attractive and brighter white color. It is observed that MPI had lower scores for L^* , a^* and b^* (47.28, 2.51, 27.14) compared with the defatted seed meal, indicating a comparatively darker protein isolate. The seed meal used for the protein isolate preparation would probably contained significant amounts of phenolics, which, on account of alkaline-induced oxidation, would result in a considerably darker protein isolate. The presence of hulls in the seed cake should not be neglected for the darkening effect. The influence of seed hulls on the browning of protein isolates was evidenced in the study of Malik *et al.*²⁸ Still, the L^* value for MPI in the present study was comparatively higher than the color results (L^* of 69.8) reported by Sadeghi and Bhagya,²⁹ which was attributed to the adopted freeze-drying method considerably reducing the oxidation-induced browning effects.

While the chroma (C) of MPI reveals the greater intensity of color as perceived by humans, the hue angle ($\tan \theta$) of MPI was 84.68°, which was lower as compared with the control (88.73°), indicating the shift in the yellow profile. Both the seed meal and protein isolate had hue angles of less than 90°, which confirms their reddish-yellow characteristic. Further, the reduced hue angle of the protein isolate indicates the efficacy of defatting and the selected alkaline pH conditions in removing the adhering pigment molecules. Similar results on increased yellow hue with increasing the pH during solubilisation extraction were reported by Wintersohle *et al.*³⁰

3.2 Physicochemical properties of native and CP-treated MPI

3.2.1 Water absorption capacity (WAC), oil holding capacity (OAC). The WAC of the native and CP-treated MPI are shown in Table 3. The WAC values ranged from 2.79 to 3.28 g g⁻¹. The WAC of the CP-treated MPI increased non-significantly ($p > 0.05$) yet proportionally to the treatments (T1, T2, and T3)

given. This non-significant increase in the ability of the CP-treated MPI to hold polar water molecules is possibly due to the presence of soluble protein fractions and polar amino groups being exposed due to the ionization process. Treating MPI with cold plasma would have generated excess reactive oxygen species, which can participate in better holding of water molecules. This is supported by the reduced pH measurements in the treated samples (6.10 g g⁻¹) as compared with the control (6.97 g g⁻¹). Treatment of native mustard protein isolate with cold plasma would have led to the generation of reactive species such as nitrous acid, nitric acid, and hydrogen peroxide radical. These generated acids likely played a key role in lowering the pH. Similar results were observed in wheat germ protein isolate by Abargheli *et al.*³¹ The increased WAC is extremely important for protein isolate gels to find application in hydrophilic food systems that contribute directly to the texture and stability of formulated foods. Additionally, the release of more free sulfhydryl groups (Section 3.4) during CP treatment would also have contributed to this increased WAC.

The OAC of the native and CP-treated MPI, presented in Table 3, ranged from 1.10 to 1.31 g g⁻¹, which is consistent with the results of Acharjee *et al.*³² The increased OAC denotes the ability of MPI to retain non-polar oil molecules against gravity, contributing significantly to the texture and mouthfeel of food products. Exposing MPI to CP increased the OAC proportionally, which might be due to unfolding and eventual exposure of non-polar hydrophobic amino acids.³³ The plasma-induced surface physical modification would have led to the development of cracks and pores, which are responsible for the entrapment of oil molecules. The microstructural patterns in the SEM images (Fig. 4) also support this uptake of water and oil molecules. However, the observed OAC value is comparatively lower than the WAC, which suggests the possible lower exposure of hydrophobic groups at the selected treatment levels. On the contrary, ultrasound treatment of MPI increased OAC at the expense of lowering the WHC.⁷

3.2.2 Emulsifying activity index (EAI) and emulsion stability index (ESI). The EAI of the native and CP-treated MPI are presented in Table 3. The EAI of the CP-treated MPI ranged from 41.25 to 47.81%, respectively, showing an increase compared with the control. The CP treatment at T2, T3 and T4 increased the EAI significantly ($p < 0.05$) compared to the control. Assessment of EAI provides insights into the interfacial properties of proteins, which is important for applications in protein-based beverage formulations and emulsified products such as ice creams and sausages.³⁴ The increased reported values are attributed to the effect of CP in reducing the interfacial tension and inducing adsorption. Our findings on

Table 2 Color profile studies of defatted mustard seed meal and mustard protein isolate^a

Sample	L^*	a^*	b^*	Chroma (C)	Hue angle (°)
Defatted mustard seed meal	53.08 ± 0.17	3.36 ± 0.017	29.84 ± 0.07	20.54 ± 0.28	88.73 ± 0.20
Mustard protein isolate	47.28 ± 1.16	2.51 ± 0.18	27.14 ± 1.42	27.26 ± 1.41	84.68 ± 0.52

^a Values are presented as mean ± standard deviation.



Table 3 Physicochemical function of native and cold-plasma-treated mustard protein isolate^a

Treatment	Water absorption capacity (g g ⁻¹)	Oil absorption capacity (g g ⁻¹)	Emulsifying activity index (%)	Emulsifying stability index (%)	Foaming capacity (%)	Foaming stability (%)
C control	2.79 ± 0.85 ^a	1.10 ± 0.06 ^a	40.06 ± 0.97 ^d	61.21 ± 2.93 ^a	51.56 ± 1.53 ^d	41.93 ± 2.85 ^a
T1 (10 kV, 5 min)	2.85 ± 0.08 ^a	1.18 ± 0.12 ^{a,b}	41.25 ± 0.72 ^d	64.13 ± 0.42 ^{a,b}	54.08 ± 0.41 ^c	42.86 ± 0.74 ^a
T2 (10 kV, 10 min)	2.90 ± 0.10 ^a	1.22 ± 0.18 ^{a,b}	43.72 ± 1.24 ^c	66.59 ± 2.15 ^{b,d,e}	56.82 ± 0.75 ^b	44.14 ± 0.68 ^a
T3 (20 kV, 5 min)	3.06 ± 0.23 ^a	1.26 ± 0.06 ^{a,b}	45.92 ± 1.26 ^b	69.55 ± 1.57 ^{b,c,d}	59.77 ± 0.39 ^b	44.68 ± 0.38 ^a
T4 (20 kV, 10 min)	3.28 ± 0.19 ^a	1.31 ± 0.05 ^a	47.81 ± 1.10 ^a	69.66 ± 1.72 ^{b,d,e}	57.30 ± 1.44 ^a	43.15 ± 1.64 ^a

^a Different superscript letters (alphabets) in the same column indicate significant differences ($p < 0.05$) level.

increased solubility (3.3) also infer that a greater distribution of polymeric chains would have made possible the movement into the interface and strengthened the emulsification. The unfolding of protein chains would have possibly neutralized the repulsive surface negative charges. In addition, the generated reactive species would have cleaved the protein intermolecular bonds, which would further lead to enhanced flexibility in the protein molecules, thereby lowering the interfacial surface tension. In a similar line of observations, Zhang *et al.*³⁵ highlighted the impact of the frequency and time duration of plasma exposure, where the group observed that treating soybean protein isolate at 80, 100 and 120 Hz for 5 and 10 min had a negative impact on the emulsion properties. On the contrary, our research was carried out at 50 Hz, which was well within the limits for improving the interfacial properties of the protein.

The ESI of the native and CP-treated MPI ranged from 61.25 to 69.11%, respectively. An increased ESI contributes to enhanced rigidity of protein molecules in maintaining a strong and durable interfacial network. The ESI of the MPI treated with T2, T3 and T4 increased significantly ($p < 0.05$) compared to the control samples (Table 3). An increase in ESI for the proteins reveals the greater stabilization potential of the polymer for the developed emulsion. The results were in agreement with the CP treatment of canola proteins by Arif *et al.* In support of this observation, our results on reduced -SH groups show that the disulfide linkages increased the stability of the emulsion.³⁶ Besides this, the increased ESI is a balance between sulphydryl groups, surface charges and induced unfolding characteristics, which altogether forms a stable aggregate capable of holding and maintaining a stronger interface. The requirement of enhanced ESI for the shelf life of food products is a prerequisite for many food products, such as dressings, sauces, ketchups and confectionary products.³⁷ In Table 3, it can be revealed that the emulsifying stability index at treatment level T3 to T4 showed a slight increase of 0.15%. This can be viewed as the start of surface-oxidation-induced aggregation, as the reactive species interact with amino acid side chains, which leads to enhanced oxidation of sulphydryl groups.³⁸ A similar observation was reported by Segat *et al.*³⁹ in whey protein isolate, where the CP treatment for 30 and 60 min induced aggregation.

3.2.3 Foaming capacity (FC) and foaming stability (FS). The FC and FS of the native and CP-treated MPI are presented in Table 3. It is observed that the FC of the treated proteins showed a significant ($p < 0.05$) increase as compared with the native MPI

and ranged from 54.08 to 59.77%, while the FS showed a non-significant ($p > 0.05$) increase. This increment in foaming capacity (FC) of CP-treated proteins to be adsorbed on to the gas/liquid interface and deliver a stable film that can resist the gravitational and mechanical forces over the bubble. Foam capacity and stability are a balance between the flexibility and molecular rigidity of protein polymers.⁴⁰ These specific properties play a key role in the formulation of aerated products and foam-based whippings.⁴¹ The partial unfolding and denaturation of protein side chains is the cause of the increased FC and FS up to T3 (20 kV for 5 min), but after this there was a slight reduction observed in the FC (4.13%) and FS (3.42%) of T4 due to the possibility of protein cohesion and aggregation.⁴² Our results on disulfide group reduction also support this obtained value. The disulfide groups confer stability, particularly in the tertiary structure, but with the T4 treatment there was a loss of stability, which would have lowered the FC and FS of the protein isolate. Similarly, Chen *et al.*⁴³ also observed a reduction in the foaming ability of egg white with an increase in sulphydryl groups over storage time. Alternatively, this could also be due to extensive oxidation induced by plasma altering the ability of protein chains to form and stabilize the interface. The success of foaming also depends on the pH of the media and the shear force it experiences during foaming.⁴⁴

3.3 Protein solubility

The protein solubility profile for native and CP-treated MPI is presented in Fig. 1. The protein solubility is an imperative and critical parameter that can drive the application of protein isolates by influencing major techno-functional characteristics such as gelling, emulsion and foaming. As the solubility factor plays a direct role in determining the denaturation or the aggregation state in food systems, evaluating this parameter is very important. The solubility (%) ranged from 57.01 to 82.08% with a significant treatment-dependent increase ($p < 0.05$). A similar increase in solubility with CP treatment was observed by Dabade *et al.*;⁴⁵ Bußler *et al.*⁴ and specifically a voltage-dependent increase in solubility was consistent with the findings of.^{42,46}

The treatments of 10 kV for 5 and 10 min and 20 kV for 5 and 10 min increased the solubility by 9.4, 24.8, 34.45, and 43.97% respectively. The increase in solubility could be attributed to the effect of reactive species generated to unfold and make a change in structural configuration, which could enable more of hydrophilic domains and thereby increase solubility. It is generally observed that the solubility profile increases in



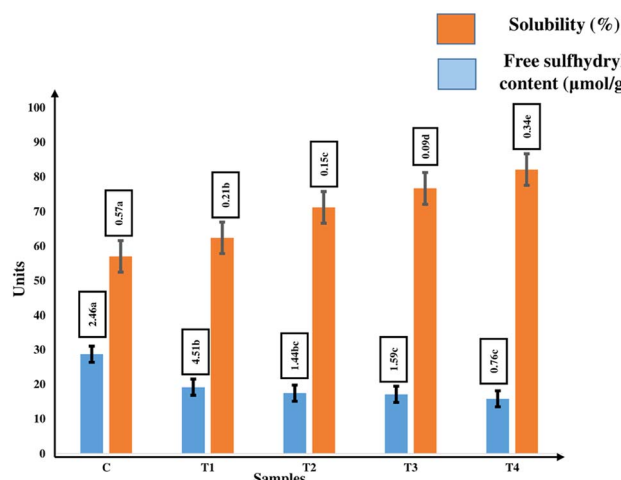


Fig. 1 Protein solubility and free sulphydryl content of native and cold-plasma-treated mustard protein isolate.

alkaline conditions and reduces close to its isoelectric point, but an extreme alkaline pH is shown to downgrade the solubility through the aggregation effect.⁴⁷ pH-shifting treatment in combination with plasma treatment was able to exceptionally increase the solubility in chickpea protein isolate.⁴⁸ This could be attributed to intermediate repulsion between the side chains followed by redistribution and increased release of soluble protein monomers. Specifically in mustard and closely related brassica species, the soluble protein contains cruciferin and napin, which have different solubility profiles. Wanasundara *et al.*⁴⁹ attempted to selectively increase the solubility of proteins in *Brassica juncea*, *Brassica napus* and *Sinapis alba* by following the salting-in approach using sodium chloride (NaCl) and calcium chloride (CaCl₂). The added salts depolymerised the major phenolic fractions and improved the solubility.

Here, the pH during the study was 7, and no major effect on solubility was observed. Employing non-thermal technologies like cold plasma can interfere with the ingredients and lead to the conversion of insoluble aggregates to a soluble form. A case of this was reported by Malik *et al.*²⁸ with ultrasound modification. In support of our obtained results, Zhang *et al.*⁵⁰ observed a solubility increase of 282% in soy protein isolate when treated at 120 kHz for 2 min. This incremental response could be due to the relatively higher frequency used to treat the native proteins. The protein solubility with the selected solvents is one of the key thermodynamic factors that possibly results in aggregation paving way for reduced solubility.⁵¹ The presence of net charges and hydrophobicity drives the solubility of proteins in suitable solvents. The etching effect of the plasma treatment and the interaction of reactive species with the protein side chains led to enhanced porosity and created active sites that can freely interact with the solvents.

3.4 Free sulphydryl groups

The free sulphydryl (–SH) group results for native and CP-treated MPI are presented in Fig. 1. The native MPI had –SH group

content of 28.74 µmol g^{−1}, which was progressively reduced with T1, T2 and T3 treatments, reaching 17.11 µmol g^{−1} (Fig. 1). The treated groups were significantly lowered ($p < 0.05$) as compared with the native MPI. This loss is expected on account of the oxidation of cysteine side chains and correlates with the observations made by Segat *et al.*³⁹ As mustard proteins tend to possess glucosinolates (β-D-glucose with sulfonium sulfonate and an R moiety) with abundant aromatic and sulfur-rich amino acids that are highly susceptible to oxidation, this reduction is inevitable. In particular, the thiol groups are easily scavenged by reactive species emanating from the plasma. Sulfenic acid, sulfenic acid, sulfonic acid and thiosulfonates are the possible end products from thiol oxidation. Besides the sulfur-rich segment, some sensitive protein chains tend to denature or unfold upon interaction with the reactive species. In practice, the reduction of reactive carbonyl and sulphydryl can be seen as a marker reaction for protein oxidation. This change in sulphydryl or carbonyl groups causes a change in the secondary structure of the protein. Here, the longer plasma exposure time increased the chances of modification through aggregation, cross-linking, and fragmentation reactions. Another possible factor could be plasma-reactive species removing or disturbing the phenol–protein conjugate in the mustard seed meal, thereby exposing more of the sensitive –SH groups.⁵² The various reactive species generated in the treated food matrix caused significant oxidative stress, particularly on the protein side chains, which was reflected in the reduction of –SH groups.

Increased disulfide linkage contributes to enhanced mechanical strength when applied to biopolymer packaging.⁵³ It is this disulfide linkage that accounted for the enhanced emulsion stability (Section 3.2.2). Further, this trend exhibited a reversal effect at T4 due to the breakdown of S–S bonds and the reduction of –SH groups. This is due to the reaction of higher energy and denser reactive species that can bombard and destroy the protein–protein linkage, thereby reducing S–S bonds. Similarly, Monica *et al.*⁵⁴ found that foxtail millet exposed to 2 kV for 25 min had a higher –SH concentration than the control group. More degradation of aggregates is attributed to the formation of –SH groups.

However, the interior –SH group gets exposed to the surface of proteins due to greater unfolding and protein dissociation, so there is a chance of a recurrent increase in disulfide formation. It could also be attributed to the impact of reactive species exposing the buried thiol groups in the interior helix. A similar effect was observed in the high-pressure treatment of rapeseed protein isolate at 200 MPa.¹⁸ An increased concentration of disulfide bonds assists in increasing the stability of the tertiary protein structure. An increased reorientation of thiol and disulfide plays a critical role in ensuring the stability of protein structure.

3.5 Thermal properties of native and treated MPI

The DSC profiles of the native and CP-treated MPI are presented in Table 4. DSC provides insight into the thermodynamic stability of isolated proteins and their thermal behaviour. The



Table 4 Thermal profile (T_d and ΔH) and relative crystallinity of native and cold-plasma-treated mustard protein isolate^a

Treatment	Denaturation temperature T_d	Enthalpy (ΔH) (J g^{-1})
C control	$91.65 \pm 0.9^{\text{a}}$	$13.68 \pm 0.14^{\text{a}}$
T1 (10 kV, 5 min)	$91.04 \pm 0.8^{\text{a}}$	$13.44 \pm 0.11^{\text{a}}$
T2 (10 kV, 10 min)	$90.07 \pm 0.03^{\text{a}}$	$13.04 \pm 0.1^{\text{a}}$
T3 (20 kV, 5 min)	$89.15 \pm 0.89^{\text{a}}$	$12.38 \pm 0.41^{\text{a}}$
T4 (20 kV, 10 min)	$89.32 \pm 0.57^{\text{a}}$	$12.94 \pm 0.44^{\text{a}}$

^a Different superscript letters (alphabets) in the same column indicate significant difference ($p < 0.05$) level.

results provide key insights into the structure and conformational changes in protein molecules. The denaturation temperature (T_d) and enthalpy (ΔH) of the native MPI were 91.65°C and 13.68 J g^{-1} , respectively. A single endothermic peak was observed in the native sample. After undergoing the CP treatment, there was a progressive reduction in the T_d and ΔH of the CP-treated MPI (T2, T3 and T4). This is in accordance with the results reported by Acharjee *et al.*³² and Dabade *et al.*⁴⁵ The reduction in T_d reflects the weakened intermolecular forces and lowered thermal stability of MPI, possibly due to the effects of unfolding and partial denaturation. An interesting observation is that, although disulfide bond (S-S) formation resumed at T4 (20 kV for 10 min), the plasma strength was insufficient to promote stronger hydrophobic interactions or induce aggregates capable of increasing the T_d .

The ΔH , which denotes the energy required for the unfolding of the orderly structure, also showed a downtrend for T1, T2 and T3. This means less energy is required for unfolding the plasma-treated protein isolate. In addition, the interaction with reactive species led to the weakening of the protein matrix and the lowering of the thermal stability. The structural deformation impact on treated MPI can be attributed to the weakening of the protein matrix and the lowering of the thermal stability. Boye *et al.*⁵⁵ proposed that the reduction in hydrophobic regions was responsible for increased WAC and reduced enthalpy. Further, in our study, with respect to T4 (20 kV for 10 min), there was a slight increase in ΔH (12.94 J g^{-1}) and T_d (89.32°C), which might be due to the enhanced aggregation of protein isolates leading to protein–protein cross-linking interactions.

3.6 FT-IR studies

The impact of CP on the secondary structure of MPI can be seen in the infrared spectrum. As observed from Fig. 2, there was no significant change in the peak position of the native and cold-plasma-treated mustard protein isolate. However, we were able to observe intensity and altitude shifts due to plasma exposure. The proteins tend to exhibit several forms, with the major ones being α helix, β sheet, β turns and random coil arrangement, which are stabilized by various covalent and non-covalent interactions. With reference to the literature, the bands detected in our study for the native and treated protein molecules can be attributed to α helix in the region of $1650\text{--}1660 \text{ cm}^{-1}$, β sheet in the regions of $1618\text{--}1640$ and $1670\text{--}1690 \text{ cm}^{-1}$, β turns in the region of $1690\text{--}1700 \text{ cm}^{-1}$ and random coils around 1645 cm^{-1} .

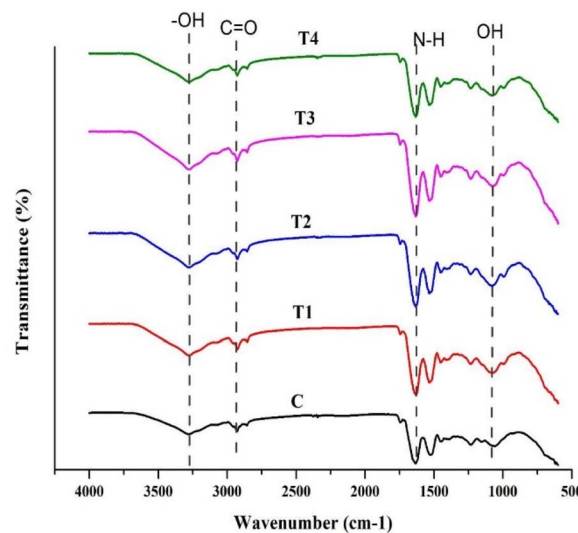


Fig. 2 FTIR spectra for native and cold-plasma-treated mustard protein isolate.

1690 cm^{-1} , β turns from 1690 to 1700 cm^{-1} , and random coils around 1645 cm^{-1} .

With regards to peptide arrangement, amide A ($3225\text{--}3280 \text{ cm}^{-1}$), amide I ($1600\text{--}1700 \text{ cm}^{-1}$), amide II ($1510\text{--}1580 \text{ cm}^{-1}$) and amide III ($1200\text{--}1300 \text{ cm}^{-1}$) can be inferred.⁵⁶ In the present study (Fig. 2), it is observed that the CP treatment had a slight impact on the secondary structure, increasing the peak intensity of the amide regions. There was a slight increment in the wavenumber for amide I, which suggests the possible release of free amino groups due to a fragmentation effect by reactive species. In addition, the amide I band occurs due to C–O stretching of the carbonyl groups, suggesting the possible effect of unfolding, denaturation and oxidation. Furthermore, our reported studies on sulphydryl groups also support this minor peak shift. The N–H bending and C–H stretching between 1510 and 1580 cm^{-1} would have led to a lowered peak signal. Additionally, there was a reduction in wavenumbers for the treated mustard protein isolates, which suggests that some of the functional groups would have interacted with reactive species. Even minor changes in amide II band can directly influence the organizational pattern. Here, it is seen that this reduction would have possibly led to reduced α helices and increased the extent of β turns and random coils. A reduction in α helix or an increase in β turns could obviously increase the flexibility of the protein chains, thereby enhancing the surface-active properties. Our findings on increased emulsification (Section 3.2.2) and foaming properties (Section 3.3.3) support this observation.⁵⁷

3.7 XRD studies

The XRD patterns for the native (C) and CP-treated MPI are presented in Fig. 3. The native MPI is characterised by three major peaks (13.6 , 19.3 , and 22.6°), the first two were smaller peaks, while the third had a higher intensity. The obtained data showed that the native MPI exhibited a partial crystalline character, while the CP-treated MPI had a pronounced broadening effect on peaks,



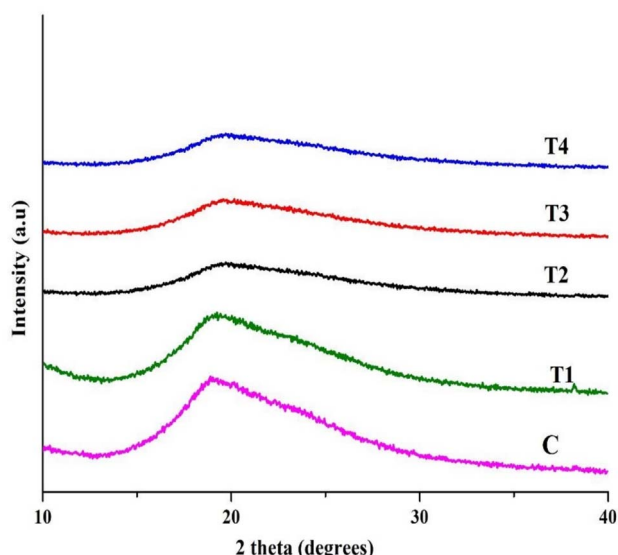


Fig. 3 XRD diffraction patterns for native and cold-plasma-treated mustard protein isolate.

leading to the lowered peak intensity. This indicates the state of aggregation and that extensive damage occurred to the native structure. The unfolding and weakening of structurally orderly molecules would have led to a loss of crystallinity in the treated samples. A similar effect on crystallinity reduction was observed by Das *et al.*⁵⁸ using a pH-shifting approach.

3.8 Microstructure studies

The SEM images of the native and CP-treated MPI at 1000 \times magnification are presented in Fig. 4. The image of the native

MPI in (i) shows the smoother surface structure and a loosely bounded nature with a compact arrangement, which was erupted and eroded by the CP treatment (T1, T2, T3, and T4), although in the control or native proteins slight eruptions were observed, which could be due to the alkali-acid treatment and subsequent drying treatment. There was a gradual loss of smooth surface and the presence of surface distortion, pores and cracks. The intensity of pores was dependent on the voltage and time of exposure to cold plasma. The T1 and T2 samples treated at 10 kV for 5 and 10 min showed the creation of numerous micropores and eventual roughness caused by etching phenomena. Specifically, the micrographs revealed the formation of a smooth T2 surface due to structural re-orientation, which made aggregation effects occurring at the surface more evident and similar effects were observed by Dong *et al.*⁵⁹ In the MPI treated at 20 kV for 5 and 10 min (T3 and T4), extensive damage occurred, which was reflected in the irregular surface arrangement. This would be due to the further extension of opened pores, creating a path for interaction with ROS and an extended etching impact. The exposed area increased the active recognition sites and severely impacted the structural homogeneity. The increased active sites were responsible for increased techno-functional properties (Section 3.2). The increase in active site formation may result in the formation of aggregates owing to oxidation. This structural impact was obviously due to the interaction of radicals with protein side chains, leading to the cleavage of C-C and C-H bonds in the peptide chains. The T3 and T4 samples would have simultaneously encountered the oxidative effect and the higher aggregation effect. Moreover, there was a weakening effect observed in the protein chains in T3 and T4, which was reflected in the reduced crystallinity. A similar trend was observed in Dabade

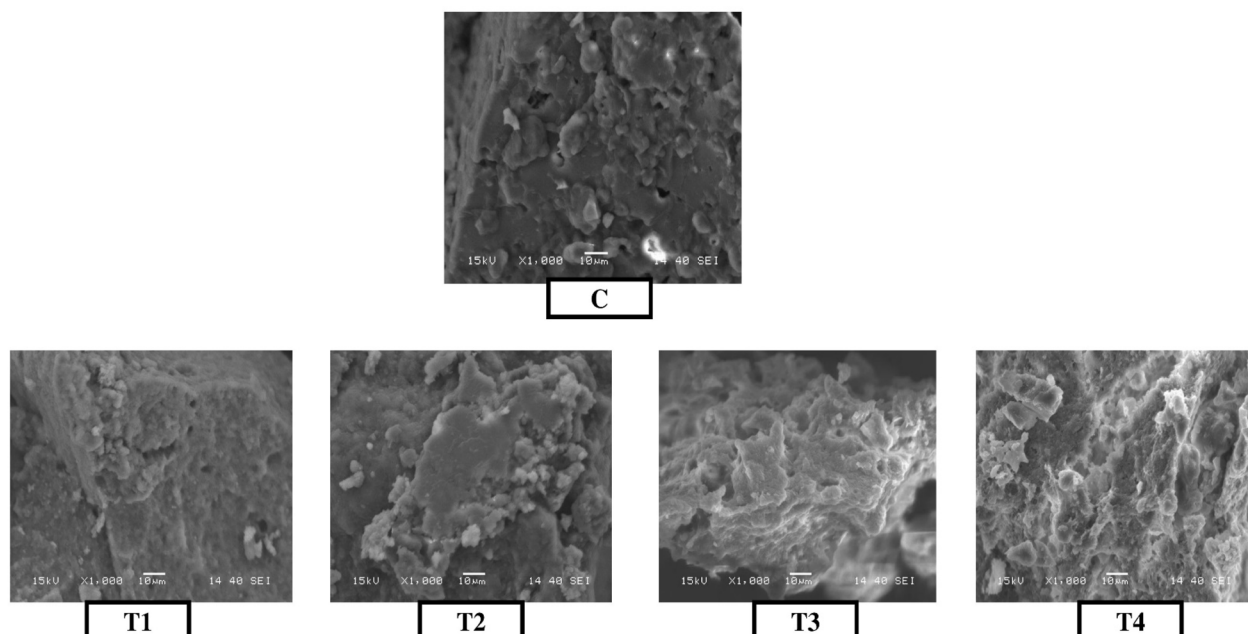


Fig. 4 SEM images of native and cold-plasma-treated mustard protein isolate.



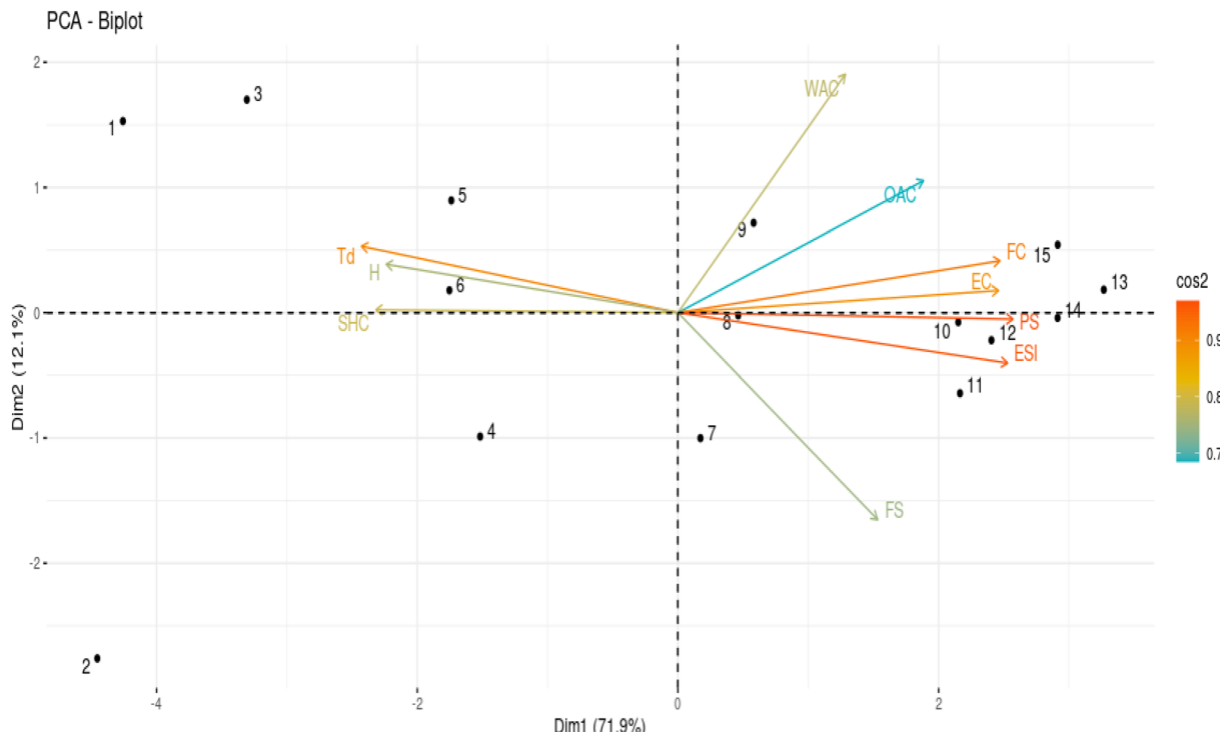


Fig. 5 PCA biplot analysis. WAC: water absorption capacity; OAC: oil absorption capacity; EC: emulsifying capacity; ESI: emulsion stability index; PS: protein solubility; FC: foaming capacity; FS: foaming stability; T_d : denaturation temperature; H : enthalpy; SHC: sulfhydryl content.

et al.⁴⁵ for the CP treatment of soy protein isolate. The CP-induced etching could result either from either the inelastic collision effect or the plasma–species interaction.

3.9 Principal component analysis

Fig. 5 depicts the principal component analysis (PCA) biplot analysis conducted for determining the effect of cold plasma treatment variation on the physicochemical, functional, and thermal characteristics of mustard protein isolate. The loading plot is denoted by red, blue and green colors, denoting the various physicochemical, functional and thermal properties, while the scalar plot in black dots represents the treatment conditions. Superimposition (0°) of loading plots on the black dots indicates a positive correlation, while a stretch in the opposite direction indicates a negative correlation. As observed from the figure, the PCA biplot explains a total of 84.0% of the total variance with two principal components: PC1 contributing 71.9% and PC2 explaining 12.1% of the variation. PC1 exhibited the highest functional properties (WAC, OAC, ES, EC, FC), whereas PC2 was associated with thermal properties (sulfhydryl groups, enthalpy). The sulfhydryl groups, enthalpy and denaturation temperature are positively correlated with the control sample. However, there was a drastic reduction in sulfhydryl groups in the native mustard protein isolate when exposed to cold plasma at T1, T2 and T3 levels. There was a treatment-dependent increase in the WAC, OAC, EC, and FC, with the treated samples performing better than the control samples. The performance reduced in the order T4 > T3 > T2 > T1 > C. As there was interaction of ROS with protein sidechains leading to

a reduction in beneficial properties, the T2 treatment (10 kV for 5 min) was positively correlated with many of the functional properties. The T3 and T4 treatments with increased voltage and duration resulted in greater protein solubility. On increasing the voltage, there was a slight reduction in foaming stability observed, which depicted a negative correlation.

4 Conclusion

The increasing interest in protein modification to meet the techno-functional requirements of the food industry has led to increased interest in utilising cold plasma technology for modifying mustard protein isolates. Accordingly, the voltage (10 kV and 20 kV) and time (5 and 10 min) of the treatment were varied to induce modification of native mustard protein isolate. The physicochemical, functional, thermal and structural properties of the treated MPI were characterised. It was observed that the treated MPI exhibited increased water absorption capacity (WAC), oil absorption capacity (OAC), emulsification and solubility profile compared with native MPI. With respect to foaming properties, there was an increasing trend observed for T1 (10 kV; 5 min), T2 (10 kV; 10 min) and T3 (20 kV; 5 min), whereas a reduction occurred in T4 (20 kV; 10 min) due to the aggregation of proteins. The aggregation behaviour was clearly observed in the microstructural studies where the reactive effect between radicals and proteins damaged the surface structure and impacted the functional performance. The excessive loss of crystallites was noticed in the reduced relative crystallinity (RC) values, indicating its negative impact on the secondary



structure of the proteins. The partial unfolding and denaturation of protein chains was observed, with a reduced temperature for denaturation and enthalpy indicating a lower thermal stability. Overall, the cold plasma treatment at 10 kV for 10 min was able to bring about balanced improvements in the physicochemical properties without severely impacting the structural conformation of the native mustard protein isolate. This modification study should contribute to the development of mustard protein isolate as a mainstream protein ingredient for application in the food, dairy and beverage segments. Further research is required to explore the effect of plasma treatment on the amino acid composition and digestibility profile of treated protein isolates.

Author contributions

Fizah Farooq (F. F.) performed the experiments. Toiba Majeed (T. M.) wrote the original manuscript. Sharath Kumar Nagaraja (S. K. N.) validated and reviewed the manuscript. Aamir Hussain Dar (A. H. D.) conceptualized and designed the study.

Conflicts of interest

The authors declare no conflict of interest.

Data availability

All data generated or analysed during this study are included in the manuscript. No new crystallographic data was generated. This study did not involve any human participants.

References

- 1 A. Das, D. P. Patel, G. C. Munda and P. K. Ghosh, Effect of organic and inorganic sources of nutrients on yield, nutrient uptake and soil fertility of maize (*Zea mays*)-mustard (*Brassica campestris*) cropping system, *Indian J. Agric. Sci.*, 2010, **80**, 85–88.
- 2 A. Paucean, S. Man, S. M. A. Pop, S. Chis and D. Cotisel, Physico-chemical and sensory properties of wheat bread supplemented with mustard flour, *Bull. UASVM Food Sci. Technol.*, 2018, **75**, 82–85.
- 3 K. M. Hendrix, M. J. Morra, H. B. Lee and S. C. Min, Defatted mustard seed meal-based biopolymer film development, *Food Hydrocoll.*, 2012, **26**, 118–125.
- 4 S. Bußler, W. B. Herppich, S. Neugart, M. Schreiner, J. Ehlbeck, S. Rohn and O. Schlüter, Impact of cold atmospheric pressure plasma on physiology and flavonol glycoside profile of peas (*Pisum sativum* 'Salamanca'), *Food Res. Int.*, 2015, **76**, 132–141.
- 5 N. S. Kumar, A. H. Dar, K. K. Dash, B. Kaur, V. K. Pandey, A. Singh and B. Kovács, Recent advances in cold plasma technology for modifications of proteins: a comprehensive review, *J. Agric. Food Res.*, 2024, 101177.
- 6 S. Sharma, Cold plasma treatment of dairy proteins in relation to functionality enhancement, *Trends Food Sci. Technol.*, 2020, **102**, 30–36.
- 7 K. Jahan, S. Fatima, K. Osama, K. Younis and O. Yousuf, Boosting protein yield from mustard (*Brassica juncea*) meal via microwave-assisted extraction and advanced optimization methods, *Biomass Convers. Biorefin.*, 2023, **13**, 16241–16251.
- 8 M. A. Sadeghi and S. Bhagya, Quality characterization of pasta enriched with mustard protein isolate, *J. Food Sci.*, 2008, **73**, S229–S237.
- 9 K. Jahan, A. Ashfaq, R. U. Islam, K. Younis and O. Yousuf, Optimization of ultrasound-assisted protein extraction from defatted mustard meal and determination of its physical, structural, and functional properties, *J. Food Process. Preserv.*, 2022, **46**, e16764.
- 10 AOAC 925.10, 65.17, 974.24, 992.16, Official Methods of Analysis of AOAC International, Maryland, USA, 2000.
- 11 J. Ge, C. X. Sun, A. Mata, H. Corke, R. Y. Gan and Y. Fang, Physicochemical and pH-dependent functional properties of proteins isolated from eight traditional Chinese beans, *Food Hydrocoll.*, 2021, **112**, 106288.
- 12 W. Ji, Y. Bao, K. Wang, L. Yin and P. Zhou, Protein changes in shrimp (*Metapenaeus ensis*) frozen stored at different temperatures and the relation to water-holding capacity, *Int. J. Food Sci. Technol.*, 2021, **56**, 3924–3937.
- 13 A. K. Stone, T. Tanaka and M. T. Nickerson, Protein quality and physicochemical properties of commercial cricket and mealworm powders, *J. Food Sci. Technol.*, 2019, **56**, 3355–3363.
- 14 H. Nawaz, M. Aslam, T. Rehman and R. Mehmood, Modification of emulsifying properties of cereal flours by blending with legume flours, *Asian J. Dairy Food Res.*, 2021, **40**, 315–320.
- 15 Y. H. Kuan and M. T. Liong, Chemical and physicochemical characterization of agrowaste fibrous materials and residues, *J. Agric. Food Chem.*, 2008, **56**, 9252–9257.
- 16 S. W. Kang, M. S. Rahman, A. N. Kim, K. Y. Lee, C. Y. Park, W. L. Kerr and S. G. Choi, Comparative study of the quality characteristics of defatted soy flour treated by supercritical carbon dioxide and organic solvent, *J. Food Sci. Technol.*, 2017, **54**, 2485–2493.
- 17 M. Barac, S. Cabrilò, M. Pesic, S. Stanojevic, S. Zilic, O. Macej and N. Ristic, Profile and functional properties of seed proteins from six pea (*Pisum sativum*) genotypes, *Int. J. Mol. Sci.*, 2010, **11**, 4973–4990.
- 18 R. He, H. Y. He, D. Chao, X. Ju and R. Aluko, Effects of high pressure and heat treatments on physicochemical and gelation properties of rapeseed protein isolate, *Food Bioprocess Technol.*, 2014, **7**, 1344–1353.
- 19 P. Kaushik, K. Dowling, S. McKnight, C. J. Barrow, B. Wang and B. Adhikari, Preparation, characterization and functional properties of flax seed protein isolate, *Food Chem.*, 2016, **197**, 212–220.
- 20 M. Hadnadev, T. Dapčević-Hadnadev, A. Lazaridou, T. Moschakis, A. M. Michaelidou, S. Popović and C. G. Biliaderis, Hempseed meal protein isolates prepared by different isolation techniques. Part I. physicochemical properties, *Food Hydrocoll.*, 2018, **79**, 526–533.



21 C. S. Saini, H. K. Sharma and L. Sharma, Thermal, structural and rheological characterization of protein isolate from sesame meal, *J. Food Meas. Char.*, 2018, **12**, 426–432.

22 A. Banerjee, S. Ganguly, N. Chatterjee and P. Dhar, Discerning the proximate composition, anti-oxidative and prebiotic properties of de-oiled meals: mustard and rice-bran, *Food Chem. Adv.*, 2023, **2**, 100247.

23 J. Pedroche, M. M. Yust, H. Lqari, J. Girón-Calle, M. Alaiz, J. Vioque and F. Millán, Brassica carinata protein isolates: chemical composition, protein characterization and improvement of functional properties by protein hydrolysis, *Food Chem.*, 2004, **88**, 337–346.

24 B. Yilmaz, T. Koçak, N. Yeşilyurt, A. Ningrum and E. N. Aksu, Mustard Meal: Marching Towards Producing a Food-Grade Protein, in *Oilseed Meal as a Sustainable Contributor to Plant-Based Protein: Paving the Way Towards Circular Economy and Nutritional Security*, Springer International Publishing, Cham, 2024, pp. 81–98.

25 M. Kaur, B. Singh, A. Kaur and N. Singh, Proximate, mineral, amino acid composition, phenolic profile, antioxidant and functional properties of oilseed cakes, *Int. J. Food Sci. Technol.*, 2021, **56**, 6732–6741.

26 N. A. Mir, C. S. Riar and S. Singh, Effect of pH and holding time on the characteristics of protein isolates from Chenopodium seeds and study of their amino acid profile and scoring, *Food Chem.*, 2019, **272**, 165–173.

27 D. N. López, R. Ingrassia, P. Busti, J. Wagner, V. Boeris and D. Spelzini, Effects of extraction pH of chia protein isolates on functional properties, *LWT*, 2018, **97**, 523–529.

28 M. A. Malik, H. K. Sharma and C. S. Saini, Effect of removal of phenolic compounds on structural and thermal properties of sunflower protein isolate, *J. Food Sci. Technol.*, 2016, **53**, 3455–3464.

29 M. A. Sadeghi and S. Bhagya, Effect of recovery method on different property of mustard protein, *World J. Dairy Food Sci.*, 2009, **4**, 100–106.

30 C. Wintersohle, I. Kracke, L. M. Ignatzy, L. Etzbach and U. Schweiggert-Weisz, Physicochemical and chemical properties of mung bean protein isolate affected by the isolation procedure, *Curr. Res. Food Sci.*, 2023, **7**, 100582.

31 M. Abarghoei, M. Goli and S. Shahi, Investigation of cold atmospheric plasma effects on functional and physicochemical properties of wheat germ protein isolate, *LWT*, 2023, **177**, 114585.

32 A. Acharjee, A. Dabade, S. Kahar and U. Annapur, Effect of atmospheric pressure non-thermal pin to plate cold plasma on structural and functional properties of pea protein isolate, *J. Agric. Food Res.*, 2023, **14**, 100821.

33 H. Sharafodin and N. Soltanizadeh, Potential application of DBD plasma technique for modifying structural and physicochemical properties of soy protein isolate, *Food Hydrocoll.*, 2022, **122**, 107077.

34 V. V. Amalia, A. D. Setiowati, I. N. A. Pratistha, M. B. P. Yudhananda, N. N. Safitri, H. N. Dewi and C. Hidayat, Formation and Performance of Red Palm Oil Emulsion Gel Stabilized by Soy Protein Concentrate–Carageenan for Animal Fat Substitute in Beef Sausage, *ACS Food Sci. Technol.*, 2025, **5**, 250–258.

35 Q. Zhang, Z. Cheng, J. Zhang, M. M. Nasiru, Y. Wang and L. Fu, Atmospheric cold plasma treatment of soybean protein isolate: insights into the structural, physicochemical, and allergenic characteristics, *J. Food Sci.*, 2021, **86**, 68–77.

36 S. Poon, A. E. Clarke and C. J. Schultz, Effect of denaturants on the emulsifying activity of proteins, *J. Agric. Food Chem.*, 2001, **49**, 281–286.

37 A. C. Karaca, N. Low and M. Nickerson, Emulsifying properties of canola and flaxseed protein isolates produced by isoelectric precipitation and salt extraction, *Food Res. Int.*, 2011, **44**, 2991–2998.

38 B. Surowsky, A. Fischer, O. Schlueter and D. Knorr, Cold plasma effects on enzyme activity in a model food system, *Innov. Food Sci. Emerg. Technol.*, 2013, **19**, 146–152.

39 A. Segat, N. N. Misra, P. J. Cullen and N. Innocente, Atmospheric pressure cold plasma (ACP) treatment of whey protein isolate model solution, *Innov. Food Sci. Emerg. Technol.*, 2015, **29**, 247–254.

40 S. Damodaran, *Food Proteins: Properties and Characterization*, 1996, pp. 167–234.

41 M. Orrego, E. Troncoso and R. N. Zúñiga, Aerated whey protein gels as new food matrices: effect of thermal treatment over microstructure and textural properties, *J. Food Eng.*, 2015, **163**, 37–44.

42 S. Jaddu, S. Sahoo, S. Sonkar, K. Alzahrani, M. Dwivedi, N. Misra and R. C. Pradhan, Cold plasma treatment of little millet flour: impact on bioactives, antinutritional factors and functional properties, *Plant Foods Hum. Nutr.*, 2024, **79**, 1–8.

43 Y. Chen, L. Sheng, M. Gouda and M. Ma, Studies on foaming and physicochemical properties of egg white during cold storage, *Colloids Surf. A*, 2019, **582**, 123916.

44 M. Aider, D. Djenane and W. B. Ounis, Amino acid composition, foaming, emulsifying properties and surface hydrophobicity of mustard protein isolate as affected by pH and NaCl, *Int. J. Food Sci. Technol.*, 2012, **47**, 1028–1036.

45 A. Dabade, S. Kahar, A. Acharjee, P. Bhushette and U. Annapur, Effect of atmospheric pressure non-thermal pin to plate cold plasma on structural and functional properties of soy protein isolate, *J. Agric. Food Res.*, 2023, **12**, 100538.

46 S. Chaple, C. Sarangapani, J. Jones, E. Carey, L. Causeret, A. Genson and P. Bourke, Effect of atmospheric cold plasma on the functional properties of whole wheat (*Triticum aestivum L.*) grain and wheat flour, *Innov. Food Sci. Emerg. Technol.*, 2020, **66**, 102529.

47 D. Gao, A. Helikh, Z. Duan and Q. Xie, Thermal, structural, and emulsifying properties of pumpkin seed protein isolate subjected to pH-shifting treatment, *J. Food Meas. Char.*, 2023, **17**, 2301–2312.

48 J. Wang, X. Zhou, J. Li, D. Pan and L. Du, Enhancing the functionalities of chickpea protein isolate through a combined strategy with pH-shifting and cold plasma treatment, *Innov. Food Sci. Emerg. Technol.*, 2024, **93**, 103607.



49 J. P. Wanasundara, S. J. Abeysekara, T. C. McIntosh and K. C. Falk, Solubility differences of major storage proteins of Brassicaceae oilseeds, *J. Am. Oil Chem. Soc.*, 2012, **89**, 869–881.

50 M. Zhang, Y. Yang and N. C. Acevedo, Effects of pre-heating soybean protein isolate and transglutaminase treatments on the properties of egg-soybean protein isolate composite gels, *Food Chem.*, 2020, **318**, 126421.

51 F. Azarikia and S. Abbasi, Mechanism of soluble complex formation of milk proteins with native gums (tragacanth and Persian gum), *Food Hydrocoll.*, 2016, **59**, 35–44.

52 M. D. Purkayastha, J. Gogoi, D. Kalita, P. Chattopadhyay, K. S. Nakhuru, D. Goyary and C. L. Mahanta, Physicochemical and functional properties of rapeseed protein isolate: influence of antinutrient removal with acidified organic solvents from rapeseed meal, *J. Agric. Food Chem.*, 2014, **62**, 7903–7914.

53 R. Thirumdas, D. Kadam and U. S. Annapure, Cold plasma: an alternative technology for the starch modification, *Food Biophys.*, 2017, **12**, 129–139.

54 V. Monica, R. Anbarasan and R. Mahendran, Cold plasma-induced changes in the structural and techno-functional properties of sprouted foxtail millet protein concentrate, *Food Bioprocess Technol.*, 2024, **18**, 850–867.

55 J. I. Boye, I. Alli and A. A. Ismail, Interactions involved in the gelation of bovine serum albumin, *J. Agric. Food Chem.*, 1996, **44**, 996–1004.

56 V. A. Lorenz-Fonfria, Infrared difference spectroscopy of proteins: from bands to bonds, *Chem. Rev.*, 2020, **120**, 3466–3576.

57 R. Thirumdas, A. Trimukhe, R. R. Deshmukh and U. S. Annapure, Functional and rheological properties of cold plasma treated rice starch, *Carbohydr. Polym.*, 2017, **157**, 1723–1731.

58 D. Das, P. S. Panesar and C. S. Saini, Effect of pH shifting on different properties of microwave-extracted soybean meal protein isolate, *Food Bioprocess Technol.*, 2024, **17**, 640–655.

59 S. Dong, P. Guo, G. Y. Chen, N. Jin and Y. Chen, Study on the atmospheric cold plasma (ACP) treatment of zein film: surface properties and cytocompatibility, *Int. J. Biol. Macromol.*, 2020, **153**, 1319–1327.

